

⁴⁸If we invoke factorization and assume that the N_2 vertices are of the same type as exist in elastic scattering, then the total cross sections can be related to the $I = \frac{1}{2}$ cross sections by the optical theorem.

⁴⁹J. G. Rushbrooke, *Nuovo Cimento Lett.* **2**, 181 (1971).

⁵⁰The use of reactions (6.4) along with data for the process $pn \rightarrow pp\pi^-$ leads to a determination of the $I = 0$ exchange amplitude in $NN \rightarrow NN\pi$. See Ref. 49.

⁵¹See, e.g., M. Jacob and G. Chew, *Strong Interaction*

Physics (Benjamin, New York, 1964), Chap. 1.

⁵²See, e.g., R. Hagedorn, *Relativistic Kinematics* (Benjamin, New York, 1963), Secs. 7-4 and 7-5.

⁵³For $M < 1.6$ GeV no off-shell corrections appear to be necessary; see Ref. 29.

⁵⁴Pion-nucleon scattering cross sections can be adequately described by the first four partial waves for $M < 1.6$ GeV; see Refs. 21 and 29.

⁵⁵E. L. Berger *et al.*, *Phys. Rev. Lett.* **20**, 964 (1968).

Measurement of the Σ^+ Magnetic Moment*

M. Saha, J. G. Fetkovich, W. Heintzelman,[†] C. Meltzer, and C. T. Murphy

Department of Physics, Carnegie-Mellon University, Pittsburgh, Pennsylvania 15213

(Received 5 January 1973)

Approximately 370 000 pictures of slow K^- interactions were taken in the Michigan-Argonne propane bubble chamber at the Argonne National Laboratory Zero-Gradient Synchrotron. They were scanned for the reaction $K^-p \rightarrow \Sigma^+\pi^-$ produced by K^- in the momentum range 250–550 MeV/c. A 45-kG magnetic field applied perpendicular to the incident beam precessed the spin of the Σ^+ through an average angle of 9° . The final sample, after cuts, consisted of 2651 events with an average time of flight of 1.5×10^{-10} sec and an average polarization of 0.37. A maximum-likelihood analysis yielded 2.7 ± 0.9 nuclear magnetons for the Σ^+ magnetic moment.

I. INTRODUCTION

SU(3) symmetry requires that the magnetic moment of the Σ^+ hyperon be equal to that of the proton, $2.79 \mu_N$, if the baryon mass differences are neglected. Bég and Pais¹ contend that this equality of magnetic moments holds only when they are expressed in units of intrinsic magnetons ($e\hbar/2m_b c$), where m_b is the mass of the baryon under considerations. In other words, their prediction for μ_{Σ^+} is $2.2 \mu_N$. Other models^{2,3} predict μ_{Σ^+} to be between 1.7 and $3.6 \mu_N$.

There have been six previous measurements⁴⁻⁹ of μ_{Σ^+} . The average of all these experiments is $\mu_{\Sigma^+} = 2.6 \pm 0.5 \mu_N$. The measurement presented here is the most precise so far.

In this experiment, polarized Σ^+ were produced in the reaction



The beam was tuned to yield K^- in the chamber ranging from 250 to 550 MeV/c to produce highly polarized Σ^+ . The Σ^+ polarization in this momentum range is well known due to the work of Kim¹⁰ and of Watson, Ferro-Luzzi, and Tripp.¹¹

II. EVENT COLLECTION

A. Exposure

The data for the present experiment were obtained from an exposure of the 40-in. Michigan-Argonne propane bubble chamber¹² to a separated K^- beam¹³ at Argonne National Laboratory. Approximately 370 000 pictures were taken with about five K^- per picture. The K^- entered the chamber with momenta in the range 450–550 MeV/c and stopped after turning through approximately 180° in the 45-kG magnetic field.

B. Scanning

Scanners were required to record all interactions of in-flight beam tracks in which two particles of opposite charge were produced, provided that the positive particle appeared to decay into a proton within 8 cm. The high stopping and trapping power of the chamber allowed rejection of most $\Sigma^+ \rightarrow n\pi^+$ decays by visual inspection; most of the decay protons stopped in the chamber. A cut of minimum length 1 cm (equivalent to one mean life) was imposed on the Σ^+ track. This

TABLE I. Hypotheses tested in the program SQUAW.

Fit No.	Reaction	Number of constraints	Unknown variable
1	$K^- + p \rightarrow \pi^- + \text{missing mass}$	0	Mass, momentum, and direction of the missing particle
2	$K^- + p \rightarrow \Sigma^+ + \pi^-$	1	Σ^+ momentum and direction
3	$K^- + p \rightarrow K^- + p$	3	Momentum of proton
4	$K^- + p \rightarrow \Sigma^+ + \pi^-$ $\quad \quad \quad \searrow$ $\quad \quad \quad p + \pi^0$	4	Σ^+ momentum, momentum and direction of π^0
5	$K^- + p \rightarrow \Sigma^+ + \pi^-$ $\quad \quad \quad \searrow$ $\quad \quad \quad n + \pi^+$	4	Σ^+ momentum, momentum and direction of n

cut reduced considerably the number of events which had to be measured. The small precession angle of the short-lived Σ^+ so rejected make them not very useful in the magnetic moment determination. Monte Carlo simulation showed that loss of these events increases the error in the magnetic moment by only 10%.

About 35% of the film was double-scanned. The average single-scan efficiency was 79% and the over-all efficiency was 85%.

C. Measurement and Data Processing

An N. R. I. microscope (film-plane digitizer) and two Vanguard image-plane digitizers were used to measure the events. Uncertainty in point reconstruction in space was about 0.25 mm in x and y .

Measured events were processed through the geometric reconstruction program TVGP¹⁴ and the kinematic fitting program SQUAW.¹⁵ Table I shows the various hypotheses tried in SQUAW. Events which failed TVGP were remeasured as many as three times, or until they could be proven not to be Σ^+ candidates on the basis of those tracks which did pass TVGP.

Events fitting hypothesis 4 (Table I) comprise the experimental sample for the measurement of μ_{Σ^+} . Some events fitting hypothesis 4 also fit hypothesis 3 or 5, indicating that they might be unwanted background. In later sections, the cuts imposed to reduce this background are discussed.

III. POLARIZATION OF THE Σ^+

To measure μ_{Σ^+} , it is necessary to know the polarization of the Σ^+ . This polarization is a

function of both E^* and θ^* , which are the energy and the production angle of the Σ^+ in the $\Sigma^+\pi^-$ rest frame, respectively. An analytic expression for this polarization is given by Kim,¹⁰ who fitted the data from several $\bar{K}N$ experiments with K^- momenta in the range 0–550 MeV/ c , using the effective-range parametrization of the K matrix formulated by Ross and Shaw.¹⁶ One might use his expression, which shows that the polarization has both positive and negative values. Alternatively, one could measure the average polarization for the entire sample, or averages for several subsamples of the data, using the observed decay asymmetry of the Σ^+ (see Sec. IV C).

In the maximum-likelihood determination of μ_{Σ^+} , we use our measured average polarization for four subsamples of the data, in order to present a model-independent result for μ_{Σ^+} . Kim's polarization is used only as a guide in forming the subsamples. Kim's fit is also used to estimate the amount of unpolarized background in our data, by comparing our measured polarizations with his predictions.

IV. BACKGROUND

A. Monte Carlo Simulation

A large number of Monte Carlo events were generated to study the effects of cuts, potential biases, and background. In the Monte Carlo program, the incident K^- momentum was set at 550 MeV/ c . The K^- was assumed to enter the chamber in a direction perpendicular to the magnetic field. Energy loss and beam attenuation resulting from decay and interactions (equivalent to an interaction length of 125 cm) were taken

into consideration. The distribution of production angle and polarization was generated using the parameters given by Kim. The length distribution was generated using the known decay time. The initial Σ^+ polarization was precessed to get the polarization at the decay vertex. The direction of the decay proton was generated according to the decay distribution

$$\begin{aligned} \frac{d\sigma}{d\Omega} &= \frac{1}{4\pi} (1 + \alpha \vec{P} \cdot \hat{n}_p) \\ &= \frac{1}{4\pi} (1 + \alpha P \cos\theta), \end{aligned} \quad (2)$$

where \vec{P} is the polarization of the Σ^+ , \hat{n}_p is the direction of motion of the decay proton, and α is the asymmetry parameter, taken to be -0.995 throughout this experiment.¹⁷

B. K^-p Elastic Scatters

Before cuts about 27% of the events fitted both hypotheses 4 and 3 (Table I). The confidence level (C. L.) distribution for fit 4 for the ambiguous events showed an excess between 0 and 10% which could be attributed to the presence of background events. Therefore all ambiguous events with C. L. for fit 4 less than 10% were excluded from the final sample. A similar excess below 5% was observed in the sample of unambiguous events. Therefore, events with C. L. < 5% were removed from the unambiguous events. Also excluded were the events with $\Sigma^+ \rightarrow p$ relative azimuth smaller than 7° , since they were found with poor efficiency and had unreliable measurements of the Σ^+ length.

The above three cuts reduced the total number of events that formed the final sample to 2651. Table II summarizes the remaining fit ambiguities. The cuts did not completely remove K^- elastic scatters from the final sample. The remaining background was estimated by two independent methods.

(i) Elastic scatters fitting hypothesis 4 should

TABLE II. Fit ambiguities in the final sample.

Sample No.	Characteristics	Number of events
1	Final sample	2651
2	K^-p elastic scatter ambiguities in sample 1	581
3	$\Sigma^+ \rightarrow \pi^+$ ambiguities in sample 1	342

have a nearly flat Σ^+ time-of-flight distribution because of the small scattering cross section. Therefore, the fraction of K^-p elastic background should be higher in long time-of-flight events. The ratios of numbers of events with time of flight above and below 4τ (τ =mean life of Σ^+) for the unambiguous, ambiguous, and Monte Carlo samples were found to be 0.062 ± 0.005 , 0.139 ± 0.015 , and 0.055 , respectively. The comparison of this ratio for the ambiguous events and the Monte Carlo sample implies an elastic-scatter background of $(1.7 \pm 0.4)\%$ left after cuts. The slight excess of long-lived events in the unambiguous sample implies a background of $(0.7 \pm 0.2)\%$ from some unknown long-lived source. Both calculations assume that the time-of-flight distribution of the background is flat. The time-of-flight distribution is shown in Fig. 1.

(ii) The second method is based on the fact that the elastic scatters should reduce the measured values of polarization. Although the proton scattered off carbon could have a left-right asymmetry, it would not contribute to the up-down asymmetry of the $\Sigma^+ \rightarrow p\pi^0$ decay. The measured value of the average polarization of the ambiguous sample was 0.48 ± 0.07 , which is in fact very close to the average value of 0.54 predicted by Kim's fit. comparison of the expected and measured polarizations for the ambiguous sample implies a contamination of 3%.

Therefore we conclude that an upper limit on elastic-scatter background in the final sample is 3%.

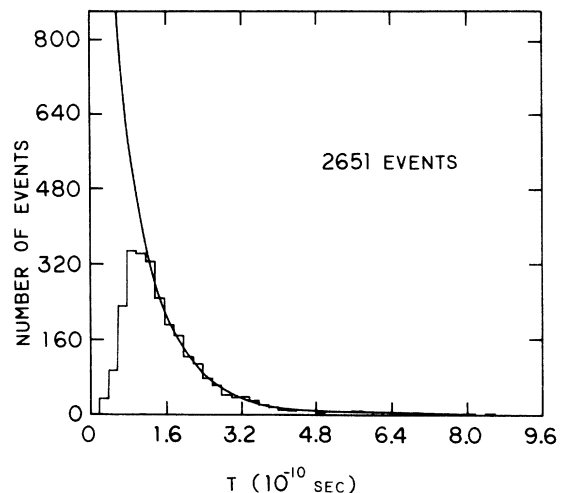


FIG. 1. Distribution of the time of flight of the Σ^+ . The solid curve is the smoothed result of the Monte Carlo program.

C. Carbon-Produced Σ^+

Many carbon-produced Σ^+ were eliminated by the restriction that there be only two outgoing tracks at the production vertex. Still others were removed when they failed to fit hypothesis 4 because of momentum imbalance. There could remain in our sample some carbon-produced Σ^+ which resulted from K^- interactions with a quasi-free proton. These events are quite usable in the measurement of the magnetic moment so long as they are similarly polarized.

To investigate this question, we compared the measured polarization of our sample with Kim's prediction. The whole sample of events was divided into four groups according to expected polarization (Kim). Table III and Fig. 2 show the results. The good agreement between measured and predicted polarizations suggests that any such background is either small or has polarization similar to the hydrogenic events. The good agreement with Kim also suggests that there are no other large sources of unpolarized background.

D. $\Sigma^+ \rightarrow \pi^+ + n$

Of the final sample of good $\Sigma^+ - p$ fits, 13% also had a good fit to $\Sigma^+ \rightarrow \pi^+ + n$ decay (Table I, hypothesis 5). We believe that nearly all of these events are $\Sigma^+ \rightarrow p$ decays, for the following reasons: Firstly, visual inspection of a small fraction of these events showed that all were identifiable as protons by ionization. Secondly, the confidence level for the $\Sigma^+ - p$ fit was usually higher than that for the $\Sigma^+ \rightarrow \pi^+$ hypothesis. Lastly, any such contamination will tend to lower the up-down asymmetry at the decay vertex, since the decay asymmetry parameter for π^+ decays is close to zero. We do not observe any such effect, as noted in Sec. IV C.

Furthermore, it is not even necessary to know the amount of unpolarized background remaining in the sample, since such a background will have no effect on the measured value of μ_{Σ^+} . This fact is demonstrated in Sec. V.

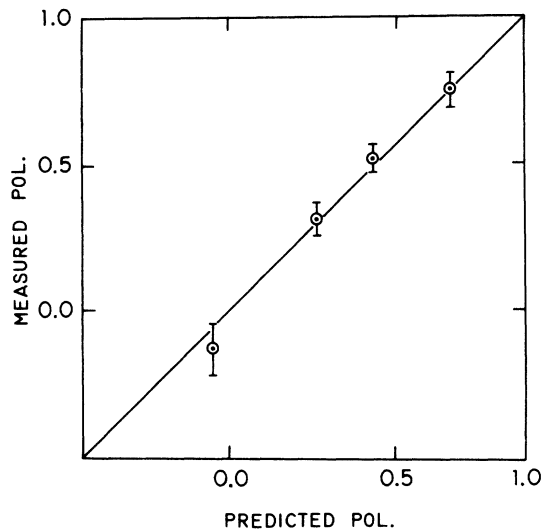


FIG. 2. The measured average polarization of four subsamples vs the average polarization for each sample predicted by Kim's analysis.

Other sources of background have been considered and found to be quite negligible. For example, Λ decay ($\Lambda \rightarrow p\pi^-$) very close to the production vertex, in which the proton scatters from carbon, would topologically resemble $\Sigma^+ - p$ decays. It was established, however, that such events would never fit hypothesis 4.

In conclusion, there is evidence for a small ($\approx 3\%$) background from K^-p elastic scatters, and an even smaller ($\sim 1\%$) long-lived background of unknown origin, and no evidence for any other sources of unpolarized background. The uncertainty in the amount of unpolarized background is included in the likelihood analysis for μ_{Σ^+} (Sec. V).

V. MAGNETIC MOMENT CALCULATION

A. Precession of Σ^+ Spin

At the production vertex, the Σ^+ spin is perpendicular to the production plane as a result of

TABLE III. Comparison between measured and Kim polarizations.

Group	Number of events	Polarization range predicted by Kim	Measured average polarization	Kim average polarization
1	324	$-1.0 \leq \text{pol.} < 0.0$	-0.13 ± 0.09	-0.05
2	851	$0.0 \leq \text{pol.} < 0.325$	0.16 ± 0.06	0.15
3	909	$0.325 \leq \text{pol.} < 0.650$	0.52 ± 0.05	0.49
4	567	$0.650 \leq \text{pol.} \leq 1.0$	0.75 ± 0.06	0.75

parity conservation. In the magnetic field, the spin precesses until decay. In the laboratory frame the time dependence of the spin four-vector is given by the following equations¹⁸:

$$\frac{dS^0}{dt} = \frac{\mu_{\Sigma} e}{m_p c} \left\{ \frac{1}{m^2 c^2} [\vec{p} \cdot (\vec{S} \times \vec{B})] p^0 \right\} - \frac{1}{m^2 c^2} \left[\left(\frac{dp^0}{dt} \right) S_0 \right] p^0, \quad (3a)$$

$$\frac{dS^i}{dt} = \frac{\mu_{\Sigma} e}{m_p c} \left\{ (\vec{S} \times \vec{B})^i + \frac{1}{m^2 c^2} [\vec{p} \cdot (\vec{S} \times \vec{B})] p^i \right\} - \frac{1}{m^2 c^2} \left[\left(\frac{dp^i}{dt} \right) S_i \right] p^i, \quad (3b)$$

where $S = (S^0, \vec{S})$ is the Σ^+ spin four-vector, $p = (p^0, \vec{p})$ is the Σ^+ momentum four-vector, B is the magnetic field strength, m_p is the mass of the proton, m is the mass of the Σ^+ , e is the charge of the Σ^+ , μ_{Σ} is the magnetic moment of the Σ^+ in nuclear magnetons, and c is the velocity of light.

B. Likelihood Analysis

Using Eqs. (3a) and (3b), we define the one-parameter likelihood function $L(\mu_{\Sigma})$ as

$$L(\mu_{\Sigma}) = \prod_i [1 + \alpha \vec{S}_{fi}(\mu_{\Sigma}) \cdot \hat{q}_i], \quad (4)$$

where \vec{S}_{fi} is the spin of the i th event at decay.

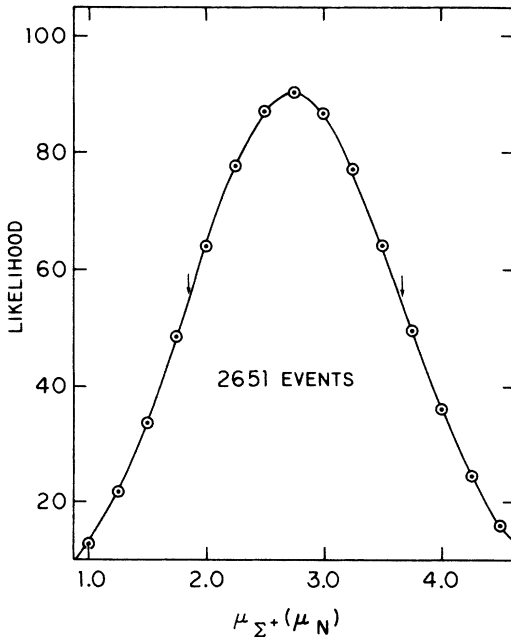


FIG. 3. The one-parameter likelihood function vs μ_{Σ^+} . This curve leads to the results of Eq. (5).

In order to make a model-independent measurement of μ_{Σ^+} , we have used our own measured values of polarization to determine \vec{S}_{fi} . As described in Sec. IV C, the Kim model was used as a guide to divide the data sample into four subsamples with different degrees of polarization (see Table III). The average polarization of each subsample was measured, and the polarization assigned to each event in the likelihood function was just the average polarization of the subsample to which the event belonged. Maximizing the likelihood function with respect to μ_{Σ^+} , we obtain

$$\mu_{\Sigma^+} = 2.74^{+0.92}_{-0.89} \mu_N. \quad (5)$$

The errors correspond to the points where $L = L_{\max} e^{-1/2}$. The likelihood function is shown in Fig. 3.

This one-parameter likelihood analysis contains the implicit assumption that the polarizations are exactly known, which is not the case. In order to investigate the effects of this uncertainty on the value and error in μ_{Σ^+} , one should perform a five-parameter likelihood analysis (four polarizations and μ_{Σ^+}) and examine the five-dimensional ellipsoids of constant likelihood for correlations. This was done by a series of two-parameter likelihood fits in which one polarization and μ_{Σ^+} were simultaneously varied. No correlations large enough to alter the error quoted in Eq. (5) by more than a few percent were found. As an example of this lack of correlations, we show in Fig. 4 the contours of constant likelihood for the two-parameter fit in which all four polarizations were varied proportionally. Specifically, the spin of each event was taken to be the average polarization of the appropriate subsample divided by $1+k$, where k is the variable second parameter of the likelihood function. The lack of correlation is apparent. The results of this two-parameter fit are

$$\mu_{\Sigma^+} = 2.73^{+0.90}_{-0.87} \mu_N, \quad (6)$$

$$k = -0.03 \pm 0.06, \quad (7)$$

$$\frac{\langle \mu k \rangle}{\Delta \mu \Delta k} = 0.02, \quad (8)$$

where $\langle \mu k \rangle$ is the correlation of k and μ_{Σ^+} evaluated on the one-standard-deviation contour.

It should be noted that replacing the polarization function \vec{S}_{fi} by an empirical average polarization for each subsample is legitimate because the polarization enters linearly in the likelihood function. By using empirical polarizations, the effect of any unpolarized background is automatically included; by allowing these polarizations to be free parameters in the likelihood analysis,

the effect of statistical uncertainties in the empirical polarizations on the error in μ_{Σ^+} is included.

We have also done maximum-likelihood analyses using the Kim polarization function for \mathfrak{S}_{ft} , and obtain results which differ negligibly from the above, as would be expected from the fact that our measured polarizations agree so well with those predicted by Kim.

VI. BIASES

There are several possible causes of bias in the experimental data. Those that have been considered are

- (1) carbon produced Σ^+ ;
- (2) $\Sigma^+ \rightarrow \pi^+ n$ decays;
- (3) long-lived background, such as $K^- p$ elastic scatters;
- (4) loss of events with small relative azimuth between the Σ^+ and the decay proton.

It has already been established in Secs. IV and V that (1) and (2) are not important. The remain-

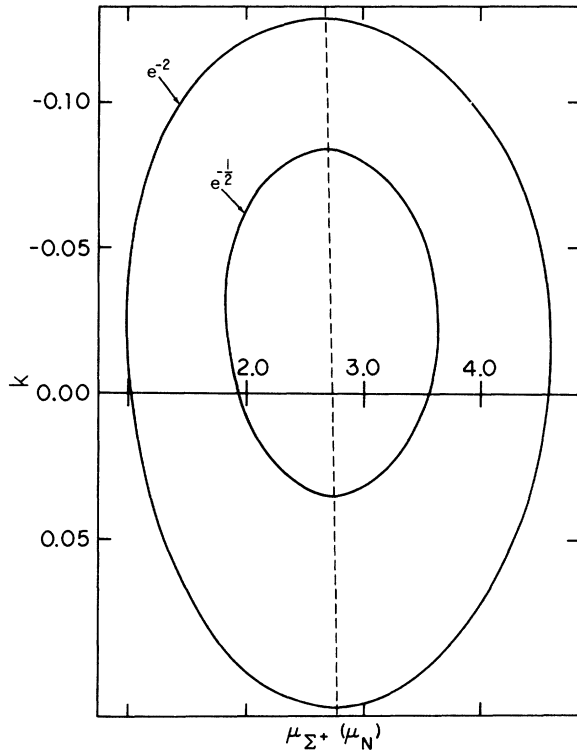


FIG. 4. Contours of constant likelihood for the two-parameter likelihood function, as a function of μ_{Σ^+} and k . The variable parameter k is the scaling factor for average polarizations, defined in the text. The contours shown are the 1- and 2-standard deviation contours ($L = L_{\max} e^{-1/2}$ and $L = L_{\max} e^{-2}$, respectively).

ing potential biases were studied using the Monte Carlo events. The Monte Carlo sample (16 000 events) was distorted to simulate these biases, and the magnetic moment of the Monte Carlo sample was then “measured” by a one-parameter likelihood method similar to that used for the real events.

The background from $K^- p$ elastic scatters, in which the proton rescatters on carbon, is another source of unpolarized background, since the proton-carbon scatter cannot have an up-down asymmetry with respect to the production plane. However, there can be a left-right asymmetry if the proton is polarized. Assuming 100% polarization and an analyzing power of 0.5 for the carbon scatter,¹⁹ we obtain 1.5% as the upper limit to the left-right asymmetry introduced in our sample from the 3% elastic scatter background. When this bias folded into the Monte Carlo sample, the “measured” magnetic moment shifted by only $0.01 \mu_N$.

To test the effect of other long-lived background, the magnetic moment was measured as a function of the time of flight of the Σ^+ (see Fig. 5). There is evidently no significant systematic trend.

The relative azimuth distribution of the data sample is shown in Fig. 6. The loss of about 30% of the events is obvious; the left-right asymmetry of the distribution is 2%. This loss could have either or both of two effects: (a) The magnetic moment measured by use of the unmodified likelihood function, Eq. (4), might be shifted relative to the value that would have been found with an unbiased sample of events; (b) the $\cos\theta$ distribution [Eq. (2)] might be distorted by the loss, resulting in an incorrect result for the error in

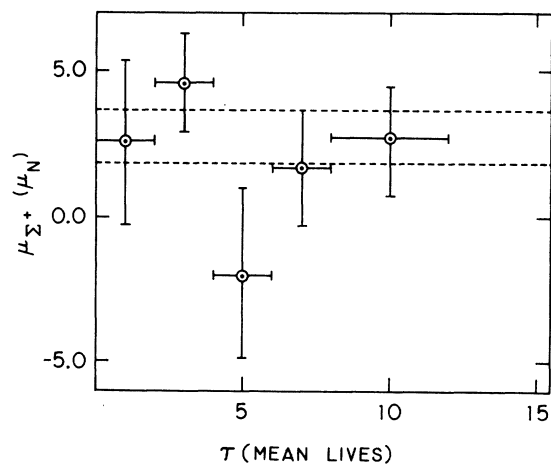


FIG. 5. The magnetic moment of the Σ^+ as a function of Σ^+ lifetime. The dashed lines show the one-standard-deviation limits of the final result for the whole sample.

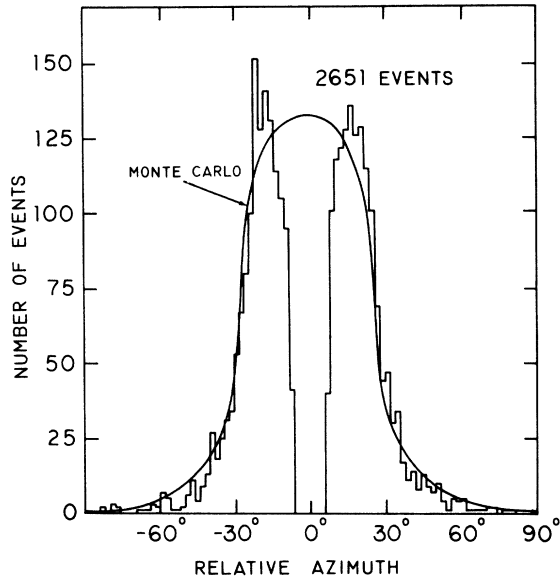


FIG. 6. Distribution of the relative azimuth between the Σ^+ and the decay proton in the lab. The curve is the smoothed prediction of the Monte Carlo program, normalized in the regions $|\text{rel. az.}| > 15^\circ$.

μ_{Σ^+} deduced from the unmodified likelihood function.

The first effect was studied by making a variety of different relative azimuth cuts (some symmetric, others asymmetric) on the Monte Carlo sample and noting the shift in the "measured" magnetic moment. The largest shift observed was $0.1 \pm 0.1 \mu_N$. No systematic trend was noticed as the cut was increased from 0° to 15° , nor when asymmetries were introduced.

The $\cos\theta$ distribution of the real events is shown in Fig. 7 and shows no signs of distortion. The distribution was fitted by the method of least squares to Eq. (4), with P set equal to the average polarization of the entire sample ($P=0.37$). The value of χ^2 was 22, with 20 degrees of freedom. There is no evidence for the need for a quadratic term.

VII. EXPERIMENTAL ERRORS

The error quoted in Eq. (6) for the magnetic moment is purely statistical. We have considered the following other sources of error which should be added to the statistical error. It was found that the 0.5% uncertainty in the value of the magnetic field and the average error of 3% in the measurement of the Σ^+ length have negligible effects on the error in μ_{Σ^+} . The error in the measurement of the angle between the Σ^+ polarization and the decay proton introduces an additional uncertainty of $0.04 \mu_N$. If this uncertainty is add-

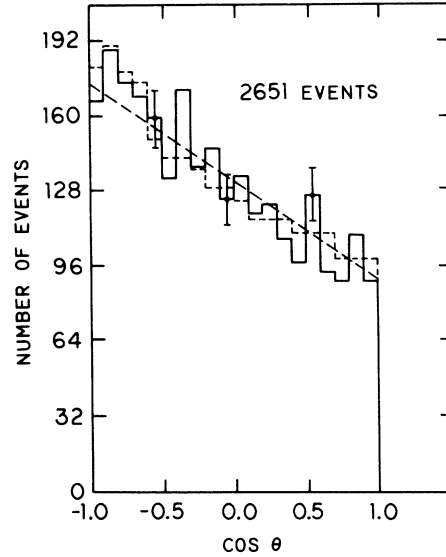


FIG. 7. The distribution of $\cos\theta$, where θ is the angle between the Σ^+ polarization and the direction of the decay proton in the rest frame of the Σ^+ . The straight line is the result of the least-squares fit to the form $N = 1 + \alpha P \cos\theta$, with αP fixed at -0.37 . The dashed histogram is the result of the Monte Carlo program.

ed in quadrature to the error quoted in Eq. (6), it also has a negligible effect.

VIII. CONCLUSION

In this experiment the magnetic moment of the Σ^+ is measured to be $2.73_{-0.87}^{+0.90}$ nuclear magnetons. The present experiment has an error slightly smaller than that of the best previous experiment. Since all the experiments agree within errors, it is appropriate to form a new weighted world average, which is $\mu_{\Sigma^+} = 2.63 \pm 0.42 \mu_N$ or 2.06 ± 0.33 sigma magnetons.

Several theoretical models have been used to calculate the magnetic moments of individual hyperons and interrelations between them. The SU(3) model of Gell-Mann and Ne'eman²⁰ predicts $\mu_{\Sigma^+} = \mu_p$. A similar model of Gürsey *et al.*,²¹ assuming integrally charged quarks, gives the same prediction. Using SU(6), Bég *et al.*¹ again make nearly the same prediction for μ_{Σ^+} . However, if the mass difference between the proton and the Σ^+ is taken into consideration, their prediction becomes $\mu_{\Sigma^+} = 2.2 \mu_N$. Using the techniques of current algebra, Mathur and Pandit³ predict $\mu_{\Sigma^+} = 3.6 \mu_N$. A dynamical model of symmetry breaking by Pagels² predicts $\mu_{\Sigma^+} = 1.7 \mu_N$.

It is evident that the world average value of μ_{Σ^+} is not consistent with either of the latter two predictions. However, the uncertainty in the mea-

sured value is not small enough to differentiate between the unbroken SU(3) prediction and the simple mass-corrected prediction of Bég. Experiments with higher accuracy are therefore necessary to differentiate between the two models.

ACKNOWLEDGMENTS

We are indebted to V. Sevcic and his bubble chamber crews for their efforts in producing a

stable, dependable bubble chamber during the exposure of this film. We thank our scanning and measuring staff for their tireless efforts, and Frank Sharkey for his programming assistance. We are especially thankful for the multiple contributions of Joe Rudman, who trained scanners, edited film, determined efficiencies, managed the data processing, and handled all bookkeeping aspects of this experiment.

*Work supported by the U. S. Atomic Energy Commission.

†Present address: Center for Naval Analyses, Arlington, Va. 22209

¹M. A. B. Bég and A. Pais, *Phys. Rev.* **137**, B1514 (1965).

²H. Pagels, *Phys. Rev.* **140**, B999 (1965).

³V. S. Mathur and L. K. Pandit, *Phys. Rev.* **147**, 965 (1966).

⁴V. Cook, T. Ewart, G. Masek, R. Orr, and E. Planter, *Phys. Rev. Lett.* **17**, 223 (1966).

⁵C. R. Sullivan, A. D. McInturff, D. Kotelchuck, and C. E. Roos, *Phys. Rev. Lett.* **18**, 1163 (1967).

⁶D. Kotelchuck, E. R. Goza, C. R. Sullivan, and C. E. Roos, *Phys. Rev. Lett.* **18**, 1166 (1967).

⁷J. Combe, E. Dahl-Jensen, N. Doble, D. Evans, L. Hoffmann, P. Rosselet, W. Toner, W. M. Gibson, K. Green, P. Tolun, N. A. Whyte, G. Charrière, M. Gailloud, B. Wanders, R. Weill, C. Carathanassis, W. Püschel, V. Scheuing, R. Settles, G. Baroni, A. Manfredini, G. Romano, and V. Rossi, *Nuovo Cimento* **57A**, 54 (1968).

⁸T. S. Mast, L. K. Gershwin, M. Alston-Garnjost, R. O. Bangerter, A. Barbaro-Galtieri, J. J. Murray, F. T. Solmitz, and R. D. Tripp, *Phys. Rev. Lett.* **20**, 1312 (1968).

⁹P. W. Alley, J. R. Benbrook, V. Cook, G. Glass, K. Green, J. F. Hague, and R. W. Williams, *Phys. Rev. D* **3**, 75 (1971).

¹⁰Jae Kim, *Phys. Rev. Lett.* **19**, 1074 (1967).

¹¹M. Watson, M. Ferro-Luzzi, and R. D. Tripp, *Phys. Rev.* **131**, 2248 (1963).

¹²B. P. Roe, D. Sinclair, and J. C. Vander Velde, in *Proceedings of the Twelfth International Conference on High-Energy Physics, Dubna, 1964*, edited by Ya. A. Smorodinskii *et al.* (Atomizdat, Moscow, 1964), Vol. 2, p. 478.

¹³A description of the beam can be found in G. Keyes, M. Derrick, T. Fields, L. G. Hyman, J. G. Fetkovich, J. McKenzie, B. Riley, and I-T. Wang, *Phys. Rev. D* **1**, 66 (1970).

¹⁴F. T. Solmitz, A. D. Johnson, and T. B. Day, Alvarez Group Programming Note No. 117, CLRL, 1965 (unpublished).

¹⁵Kinematic fitting program written by T. B. Day, O. I. Dahl, and F. T. Solmitz (unpublished).

¹⁶M. Ross and G. Shaw, *Ann. Phys. (N.Y.)* **13**, 147 (1961).

¹⁷A. Barbaro-Galtieri, S. E. Derenzo, L. R. Price, A. Rittenberg, A. H. Rosenfeld, N. Barash-Schmidt, C. Bricman, M. Roos, P. Söding, and C. G. Wohl, *Rev. Mod. Phys.* **42**, 98 (1970).

¹⁸M. Saha, Ph.D. thesis, Carnegie-Mellon University, 1972 (unpublished).

¹⁹V. Z. Peterson, University of California Report No. UCRL-10622, 1963 (unpublished).

²⁰S. Coleman and S. L. Glashow, *Phys. Rev. Lett.* **6**, 423 (1961).

²¹F. Gürsey, T. D. Lee, and M. Nauenberg, *Phys. Rev.* **135**, B467 (1964).